ELSEVIER

Contents lists available at ScienceDirect

International Journal of Particle Therapy

journal homepage: www.sciencedirect.com/journal/ijpt



Cardiac Substructure Dose Reduction and Toxicity Risk Assessment: IMPT Versus IMRT for Breast Cancer



Lu Cao (PhD, MD)^{1,2,†}, Han Zhao (BS)^{1,2,†}, Shujun Zhang (MS)^{1,2,†}, Keman Liao (PhD, MD)^{1,2,†}, Mei Chen (MS)^{1,2}, Gang Cai (MD)^{1,2}, Dan Ou (MD)^{1,2}, Jing Yang (MD)^{1,2}, Xiaoyu Wu (MD)^{1,2}, Huan Li (MD)^{1,2}, Feifei Xu (MD)^{1,2}, Weixiang Qi (MD)^{1,2,‡}, Yibin Zhang (BS)^{1,2}, Jiayi Chen (PhD, MD)^{1,2,*}

ARTICLE INFO

Keywords:
Intensity-modulated proton therapy
Radiation dose
Cardiac substructures
Normal Tissue Complication Probability model
Cardiac toxicity

ABSTRACT

Purpose: Intensity-modulated proton therapy (IMPT) significantly reduces mean heart dose (MHD), but data on cardiac substructure dose and toxicity compared to intensity-modulated radiation therapy (IMRT) are limited. This study evaluated dose reduction in cardiac substructures between IMPT and IMRT and assessed cardiac toxicity risks using 2 normal tissue complication probability models.

Materials and methods: A retrospective analysis was conducted on 30 breast cancer patients from a randomized trial with the highest MHD receiving IMRT. IMPT plans were created for a prescribed dose of 4005 cGy(RBE) in 15 fractions. Normal tissue complication probability models were used to compare individual acute coronary events (ACEs) risk between IMPT and IMRT.

Results: Intensity-modulated proton therapy reduced cardiac substructure doses by 63.34% to 100%, with greater absolute reductions in left-sided and relative reductions in right-sided patients. For left-sided internal mammary node irradiation (IMNI), IMPT achieved an 82.25% reduction for left anterior descending coronary artery (P=.009), 79.45% for RV (P<.001), and over 90% for other substructures. Right-sided patients had near-zero mean doses in most substructures. The Darby model indicates IMPT reduces individual ACE risk by 1.58% to 5.16% for left-sided IMNI (P=.001) and 0.59% to 1.05% for right-sided IMNI (P=.063). The Bogaard model shows a 0.19% to 2.75% reduction in individual 9-year ACE risk-based MHD for left-sided IMNI (P=.0015). Risk reduction variations are influenced by dose reduction and other risk factors.

Conclusion: Intensity-modulated proton therapy provides excellent cardiac protection, particularly for left-sided IMNI and high-risk patients.

Introduction

Breast cancer is one of the most prevalent malignancies affecting women globally, with radiation therapy (RT) playing a crucial therapeutic role. ^{1.4} While RT effectively reduces local recurrence and improves survival in breast cancer, it also raises concerns about cardiac toxicity, which could compromise the survival benefits. ^{2,5-7} There is no established safe threshold for cardiac radiation exposure, although minimizing cardiac doses has been continuously recommended. ⁸⁻¹¹ Novel RT techniques for

breast cancer have prioritized minimizing cardiac exposure, such as heart-sparing techniques, deep inspiration breath-hold, and image-guided radiation therapy. ^{6,12} Particle therapy, in particular proton therapy, with its unique physical aspects, offers superior cardiac dose reduction than photon therapy. ¹³⁻¹⁹ Other particles, such as carbon ions, have shown their perspective not only in reducing cardiac dose reduction but also in improving therapeutic outcomes. ¹⁴⁻¹⁷

Despite the dosimetric advantages of proton therapy in sparing the heart, its correlation to cardiac event reduction remains to be defined in

Department of Radiation Oncology, Ruijin Hospital, Shanghai Jiaotong University School of Medicine, Shanghai, China

² Shanghai Key Laboratory of Proton Therapy, Shanghai, China

^{*} Corresponding author. Department of Radiation Oncology, Ruijin Hospital, Shanghai Jiaotong University School of Medicine, 197 Ruijin Second Road, Shanghai 200025, China.

E-mail addresses: qwx12055@rjh.com.cn (W. Qi), cjy11756@rjh.com.cn, chenjiayi0188@aliyun.com (J. Chen).

Equal contribution.

^{*} Weixiang Qi is responsible for statistical analysis.

breast cancer. 18-21 There are ongoing Phase III trials, such as RADCOMP and DBCG Proton, assessing the efficacy of cardiac protection with proton therapy in patients with a high risk of cardiac toxicity. ^{22,23} Using the Normal Tissue Complication Probability (NTCP) model developed by Darby et al,8 the national proton therapy working group for breast cancer in the Netherlands established a threshold value of a 2% absolute reduction in the risk of acute coronary events (ACEs) as a criterion for proton therapy recommendation, which also becomes a basis for its reimbursement since January 2019.²⁴ These studies primarily estimate the clinical benefits of proton therapy based on the reduction in dose to the whole heart. Modern RT techniques, like intensity-modulated radiation therapy (IMRT), show considerable variability in dose distribution across cardiac substructures. 25-29 Our previous study demonstrated that the left anterior descending coronary artery (LAD), left ventricle (LV), and right ventricle (RV) receive the highest doses for left-sided patients and right atrium (RA), right coronary artery (RCA), and RV were most irradiated for right-sided patients.²⁹ The difference in radiosensitivity and corresponding clinical manifestation of cardiac substructures adds complexity to assessing radiation-induced cardiac toxicity beyond LV dysfunctions and coronary artery disease. 25,2

With the background that intensity-modulated proton therapy (IMPT) has significantly reduced whole heart dose in breast cancer patients compared to any of the photon RT techniques, the current study aims first to provide a panorama view of differences in cardiac substructure doses between IMPT and IMRT in patients with different tumor laterality and target volume, second, to compare the possible associated risks of cardiac toxicity based on 2 NTCP models.

Materials and methods

Study population

A total of 199 patients enrolled in a randomized trial²⁹ that evaluated early cardiac toxicity in breast cancer patients receiving postoperative IMRT under free breathing were retrospectively reviewed. This trial allowed hypofractionated and conventional regimens. Patients were classified into 6 groups based on the tumor laterality and target volume: left-sided whole breast irradiation (WBI), left-sided regional nodal irradiation (RNI) without internal mammary node irradiation (IMNI), left-sided RNI with IMNI, right-sided WBI, right-sided RNI without IMNI, and right-sided RNI with IMNI. Patients receiving RNI also underwent WBI or chest wall irradiation. For this study, we renormalized the treated IMRT plans to 4005 cGy in 15 fractions, and the boost plans for the tumor bed were excluded. The heart was contoured according to the atlas published by Feng et al,34 and mean heart dose (MHD) was calculated. The 5 patients with the highest MHD from each group were selected. In total, 30 patients were enrolled in this analysis. This study was approved by the local ethics committees of the participating institutions, and informed consent was obtained from all patients.

Treatment planning

Patients were immobilized on a breastboard (Klarity) and positioned in a supine position with both arms abducted over the head. All CT scans were acquired in the helical mode under free breathing. Clinical target volumes (CTVs) of the whole breast and chest wall were contoured following the Radiation Therapy Oncology Group guidelines, ³⁵ with specific modifications to the anterior and posterior CTV borders. These modifications limited the extension to 3 to 5 mm subcutaneously and excluded the ribs and intercostal muscles. The regional lymph nodes were delineated as in our previous report. ³⁶

For the IMRT planning, the planning target volume was created by expanding the CTV by an isotropic margin of 5 mm. Treatment plans were designed using a fixed-jaw IMRT technique³⁷ in the Eclipse treatment planning system (Version 13.6 and 15.6, Varian Medical

Systems, Palo Alto, CA). A 3 mm bolus was introduced for chest wall irradiation. We used the analytical anisotropic algorithm for dose calculation. For the IMPT planning, plans were created using 2 to 3 beams with a 4.67 g/cm² range shifter in the RayStation treatment planning system (Version 10B, RaySearch Laboratories AB, Stockholm, Sweden). A constant relative biological effectiveness (RBE) of 1.1 was adopted. Plans were robustly optimized to fulfill the CTV coverage, considering 3 mm setup uncertainties in 3 dimensions and 3.5% range uncertainty. The Monte Carlo algorithm was used in the dose optimization and final dose calculation. The end-of-range LET effects were not explicitly modeled during IMPT optimization, and LET-based optimization was not utilized. The IMRT and IMPT plans were normalized to cover 95% of the CTV with the 4005 cGy (RBE). Planning directives are detailed in the Supplement materials.

Data collection

The delineation of cardiac substructures, including the LV, left atrium, RA, RV, LAD, RCA, left circumflex coronary artery (LCX), and left main coronary artery (LM), followed the heart atlas by Feng et al. ³⁴ Dosimetric parameters for the heart and cardiac substructures were collected for both IMRT and IMPT plans. Additionally, patient demographics, cardiac risk factors, tumor characteristics, and treatment data were collected for analysis.

Estimation of cardiac toxicity

The risk of cardiac toxicity was assessed using the established NTCP models. The Darby et al 8 model estimates a 7.4% relative increase of ACE risk per Gy of MHD. According to the national indication protocol for proton therapy in the Netherlands, the absolute lifetime risk of ACE in our cohort was calculated by applying this model to the Dutch absolute incidence of ACE, adjusting for gender, age, and cardiovascular risk factors including previous ischemic cardiovascular disease, any previous "circulatory disease" other than ischemic cardiovascular disease, diabetes, chronic obstructive pulmonary disease, active smoker, body mass index $\geq 30 \text{ kg/m}^2$, and chronic pain medication. 24 In addition, we also applied the van den Bogaard et al 38 model, which calculated the ACE risk within 9 years based on MHD or the volume of the LV receiving 5 Gy (LV_V5). This model incorporates a weighted ACE risk score that accounts for individual cardiovascular risk factors, including diabetes, hypertension, and previous ischemic cardiac events.

Statistical analysis

Continuous variables were summarized using means and standard deviations or medians and ranges. Categorical variables were described with frequencies and percentages. To compare dosimetric parameters and the ACE risk between IMPT and IMRT plans, paired t-tests or Wilcoxon signed-rank tests were used. Spearman's correlation coefficients were calculated to analyze the inter-parameter relationships of percentage reductions in dosimetric values of the whole heart and cardiac substructures when comparing IMPT plans to IMRT plans. These correlations were visualized with a heatmap to highlight significant associations and patterns. Statistical significance was defined as 2-sided P < .05. Analyses were conducted using SPSS version 25.0 (IBM Corporation, USA), R version 4.3.2 (R Foundation for Statistical Computing, Vienna, Austria), and GraphPad Prism 6 (GraphPad Software, La Jolla, CA).

Results

Patient characteristic

Demographics, tumor, and treatment information are detailed in Table 1. In the 30 patients, the median age is 54 years, ranging from 33 to 79. Most patients (80%) had no cardiovascular risk factors.

Table 1Patient demographics, tumor characteristics, and treatment details.

Parameters	N	%	
Age (y), median (range)	54 (33-		
No. of cardiovascular risk factors	79)		
0	24	80.0%	
≥1	6	20.0%	
History of cardiovascular comorbidity			
Ischemic heart disease			
No	30	100.0%	
Yes	0	0.0%	
Hypertension No	25	83.3%	
Yes	5	16.7%	
Diabetes	3	10.7 /	
No	29	96.7%	
Yes	1	3.3%	
Other circulatory disease			
No	29	96.7%	
Yes	1	3.3%	
COPD			
No	30	100.0%	
Yes	0	0.0%	
Lifestyle risk factors			
BMI $\geq 30 \text{ kg/m}^2$	20	06 70/	
No Yes	29 1	96.7% 3.3%	
Current smoker	1	3.3%	
No	30	100.0%	
Yes	0	0.0%	
T stage ^a	· ·	0.070	
T1	17	56.7%	
$T \ge 2$	13	43.3%	
N stage			
N0	11	36.7%	
N1	13	43.3%	
N2	4	13.3%	
N3	2	6.7%	
HR status	_		
Negative	5	16.7%	
Positive	25	83.3%	
HER2 status Negative	23	76.7%	
Positive	23 7	23.3%	
Primary surgery	,	23.370	
Mastectomy	13	43.3%	
BCS	17	56.7%	
ALND			
No	13	43.3%	
Yes	17	56.7%	
Chemotherapy			
Neoadjuvant + Adjuvant	2	6.7%	
Adjuvant	20	66.7%	
None	8	26.7%	
Chemotherapy regimens			
Anthracyclines	2	6.7%	
Taxanes	8	26.7%	
Anthracyclines + Taxanes	20	66.7%	
HER2-targeted therapy in HER2-positive tumor $(N = 7)$			
(N = 7) No	0	0.0%	
Yes	7	100.0%	
Endocrine therapy in HR-positive tumor	•	100.070	
(N = 25)			
No	0	0.0%	
Yes	25	100.0%	

Abbreviations: COPD, chronic obstructive pulmonary disease; BMI, body mass index; HR status, hormone receptor status; HER2 status, human epidermal growth factor receptor 2 status; BCS, breast-conserving surgery; ALND, axillary lymph node dissection.

Hypertension was observed in 16.7% of the cohort, and diabetes and other circulatory diseases were present in 3.3% each. No patients had ischemic heart disease or chronic obstructive pulmonary disease. Only 1 patient (3.3%) had a body mass index $\geq 30~kg/m^2$. Chemotherapy was given to 73.4% of patients, featuring regimens with anthracyclines, taxanes, or a combination thereof. All HER2-positive patients received targeted therapy, and all HR-positive patients received endocrine therapy.

Reduction in dose to the whole heart with intensity-modulated proton therapy compared to intensity-modulated radiation therapy

IMPT significantly reduces radiation exposure to the whole heart compared to IMRT (Table 2). For left-sided WBI, MHD was lowered from 434.83 \pm 38.07 cGy with IMRT to 31.09 \pm 8.57 cGy(RBE) with IMPT, a magnitude of 92.83% (P<.001). In left-sided RNI without IMNI, MHD was 424.28 \pm 60.05 cGy with IMRT and 66.31 \pm 25.88 cGy(RBE) with IMPT, an 84.71% decrease (P<.001). With IMNI, IMPT reduces MHD from 563.31 \pm 65.28 cGy with IMRT to 76.97 \pm 10.62 cGy(RBE), an 86.74% reduction (P=.007). Across dose-volume parameters (maximum dose, V2, V5, V10, V15, V25, V30), IMPT consistently reduces cardiac exposure (all P<.05). For right-sided patients, IMPT also effectively decreases radiation exposure to the whole heart, with V2, V5, V10, V15, V25, and V30 close to 0.

Reduction in dose to cardiac substructures with intensity-modulated proton therapy compared to intensity-modulated radiation therapy

The irradiation fields and isodose distribution diagrams of IMRT and IMPT are shown in Figure 1A. IMPT significantly reduces mean doses to all cardiac substructures compared to IMRT (Figure 1B and C, Figure 2, and Table S1). For left-sided WBI with IMPT, mean doses to the LA, RA, RCA, and LM were lowered to almost zero (all P < .001), and nearly 100% reduction in LCX (P = .063). In left-sided RNI without IMNI, a reduction of over 90% was observed in all substructures except for LAD, which was a 63.34% reduction. With IMNI, IMPT achieves an 82.25% reduction for LAD (P = .009), 79.45% for RV (P < .001), and over 90% for other substructures (Figures 1B and 2A and Table S1). For right-sided patients, nearly zero mean dose was found in all substructures, with only limited maximum dose to the RA, RV, and RCA found in RNI with IMNI (Figures 1C and 2B and Table S1). The remaining dose for IMPT was concentrated to LAD, with mean doses of 356.47 ± 144.87 cGy(RBE), 455.44 ± 307.28 cGy(RBE), and 478.84 ± 396.77 cGy(RBE) for WBI, RNI without IMNI, and RNI with IMNI, respectively (Figure 3). No significant correlation between whole heart dose and substructures dose reduction for both left- and rightsided patients was found (Figure S1).

IMPT also significantly reduces the maximum dose to cardiac substructures compared to IMRT (Figure S2 and Table S2). With IMPT, the remaining maximum doses were concentrated to the LV, RV, and LAD in left-sided patients, and to the RA, RV, and RCA in right-sided RNI with IMNI (Figure S3). No significant correlation between whole heart maximum dose and substructures maximum dose reduction for both left- and right-sided patients either (Figure S4).

Reduction in estimated acute coronary event risk with intensity-modulated proton therapy compared to intensity-modulated radiation therapy

Both the Darby model and the Bogaard model show significant benefits of IMPT over IMRT in reducing ACE risk, particularly for left-sided patients (Figure 4 and Table S3). Using the Darby model, IMPT reduces individual ACE risk by 1.58% to 5.16% for left-sided RNI with IMNI (P=.001) and 0.59% to 1.05% for right-sided RNI with IMNI (P=.063), based on cardiovascular risk factors. Using the Bogaard model, IMPT reduces ACE risk within 9 years. However, prediction

^a The staging adhered to the seventh edition American Joint Committee on Cancer (AJCC) staging system and recorded the maximal disease stage in patients receiving neoadjuvant therapy.

Table 2
Comparisons of dosimetric parameters for the whole heart between IMRT and IMPT.

	IMRT	IMPT	Absolute decrease		Percentage decrease (%)		
	Mean ± SD	Mean ± SD	Median	Range	Median	Range	P
Left-sided WBI							
Heart_Dmean (cGy[RBE])	434.83 ± 38.07	31.09 ± 8.57	409.76	354.29-459.65	92.83	90.57-95.30	< .001
Heart_Dmax (cGy[RBE])	4151.63 ± 138.55	2982.18 ± 456.84	1052.43	673.29-1628.02	24.89	15.61-39.02	.003
Heart_V2 (%)	35.53 ± 4.53	3.28 ± 0.61	33.53	26.28-37.07	90.39	89.40-92.92	< .001
Heart_V5 (%)	13.73 ± 0.98	1.84 ± 0.53	11.80	11.25-12.90	87.81	82.24-89.69	< .001
Heart_V10 (%)	9.64 ± 0.82	0.91 ± 0.40	8.60	7.62-10.22	91.01	85.49-94.76	< .001
Heart_V15 (%)	8.10 ± 1.22	0.44 ± 0.28	7.49	6.18-9.54	94.20	89.52-97.84	< .001
Heart_V25 (%)	6.08 ± 1.59	0.05 ± 0.10	5.77	3.83-7.97	99.77	96.17-99.99	.001
Heart_V30 (%)	5.23 ± 1.67	0.01 ± 0.03	4.89	2.84-7.09	100.00	98.57-100.00	.002
Left-sided RNI without IMNI							
Heart_Dmean (cGy[RBE])	424.28 ± 60.05	66.31 ± 25.88	352.26	325.80-407.50	84.71	80.82-91.42	< .001
Heart_Dmax (cGy[RBE])	4313.74 ± 169.42	3450.77 ± 469.99	654.58	410.40-1763.24	15.96	9.83-39.58	.027
Heart_V2 (%)	33.47 ± 14.88	5.28 ± 1.71	22.18	16.67-46.64	83.89	79.48-87.19	.009
Heart_V5 (%)	14.83 ± 3.56	3.39 ± 1.38	11.59	7.95-15.50	79.45	70.48-83.84	.001
Heart_V10 (%)	10.79 ± 2.42	2.09 ± 0.99	8.88	6.69-11.95	85.20	69.37-90.44	.001
Heart_V15 (%)	8.31 ± 1.48	1.38 ± 0.72	6.59	5.51-8.67	80.60	74.30-95.52	< .001
Heart V25 (%)	5.47 ± 1.15	0.50 ± 0.32	5.59	3.61-6.08	87.48	85.18-99.84	.001
Heart V30 (%)	3.82 ± 1.48	0.20 ± 0.16	3.16	1.75-5.27	92.49	91.90-100.00	.005
Left-sided RNI with IMNI	3.02 _ 1.10	0.20 _ 0.10	5.10	1.70 0.27	52.15	31.90 100.00	.005
Heart_Dmean (cGy[RBE])	563.31 ± 65.28	76.97 ± 10.62	458.69	442.41-600.57	86.74	82.86-89.03	.007
Heart_Dmax (cGy[RBE])	4393.07 ± 210.52	3474.29 ± 300.47	1061.62	236.43-1335.83	24.85	5.70-28.42	.008
Heart V2 (%)	44.09 ± 13.26	8.39 ± 0.79	35.85	20.58-55.50	82.98	68.93-86.25	.004
Heart_V5 (%)	23.08 ± 6.36	4.79 ± 0.81	17.32	12.17-25.58	78.33	71.47-85.64	.004
	13.41 ± 2.05	2.20 ± 1.07	9.99	8.45-14.82	86.42	69.39-92.30	.002
Heart_V10 (%)			9.99 9.79				
Heart_V15 (%)	11.22 ± 2.60	0.91 ± 0.71		6.28-13.65	94.80	78.18-98.24	.002
Heart_V25 (%)	8.79 ± 2.88	0.10 ± 0.09	8.40	4.63-11.61	99.42	96.76-99.87	.003
Heart_V30 (%)	6.86 ± 2.62	0.02 ± 0.03	7.45	3.33-9.34	99.86	98.43-99.96	.004
Right-sided WBI	01.05 + 00.60	0.01 + 1.00	00.70	05 07 101 40	07.01	00.07.00.07	060
Heart_Dmean (cGy[RBE])	81.95 ± 29.62	2.01 ± 1.88	89.78	25.07-101.49	97.91	83.07-99.87	.063
Heart_Dmax (cGy[RBE])	917.85 ± 550.92	284.52 ± 163.29	490.71	-74.90 to 1547.97	67.29	-20.50 to 94.98	.087
Heart_V2 (%)	5.52 ± 3.49	0.03 ± 0.04	5.54	0.42-10.16	99.90	79.96-100.00	.025
Heart_V5 (%)	0.25 ± 0.35	0.00 ± 0.00	0.03	0.00-0.76	100.00	100.00-100.00	.177
Heart_V10 (%)	0.03 ± 0.06	0.00 ± 0.00	0.00	0.00-0.15	100.00	100.00-100.00	.371
Heart_V15 (%)	0.00 ± 0.01	0.00 ± 0.00	0.00	0.00-0.01	100.00	100.00-100.00	1.000
Heart_V25 (%)	0.00 ± 0.00	0.00 ± 0.00	0.00	0.00-0.00	100.00	100.00-100.00	/
Heart_V30 (%)	0.00 ± 0.00	0.00 ± 0.00	0.00	0.00-0.00	100.00	100.00-100.00	/
Right-sided RNI without IMNI							
Heart_Dmean (cGy[RBE])	173.14 ± 32.83	3.47 ± 2.08	175.08	119.49-203.38	98.21	96.71-99.12	< .001
Heart_Dmax (cGy[RBE])	1716.22 ± 1197.37	614.59 ± 478.36	895.32	358.50-2463.52	66.72	32.31-84.36	.038
Heart_V2 (%)	24.47 ± 4.20	0.14 ± 0.25	24.54	18.03-27.99	99.76	97.98-100.00	< .001
Heart_V5 (%)	6.33 ± 3.90	0.03 ± 0.06	6.17	1.16-10.59	100.00	97.87-100.00	.023
Heart_V10 (%)	0.60 ± 0.97	0.00 ± 0.00	0.22	0.00-2.30	100.00	99.65-100.00	.063
Heart_V15 (%)	0.30 ± 0.67	0.00 ± 0.00	0.00	0.00-1.49	100.00	100.00-100.00	1.000
Heart_V25 (%)	0.12 ± 0.26	0.00 ± 0.00	0.00	0.00-0.59	100.00	100.00-100.00	1.000
Heart_V30 (%)	0.05 ± 0.12	0.00 ± 0.00	0.00	0.00-0.27	100.00	100.00-100.00	1.000
Right-sided RNI with IMNI							
Heart_Dmean (cGy[RBE])	224.64 ± 10.03	22.12 ± 5.36	205.69	191.65-212.09	90.72	86.42-92.37	< .001
Heart_Dmax (cGy[RBE])	3187.72 ± 468.93	1548.74 ± 522.63	1613.31	745.65-2714.79	45.61	30.29-74.54	.011
Heart_V2 (%)	35.64 ± 5.49	2.85 ± 0.76	35.07	25.24-39.46	92.23	88.17-94.62	< .001
Heart_V5 (%)	8.10 ± 3.50	0.81 ± 0.71	6.49	2.93-12.33	92.28	60.07-97.88	.014
Heart_V10 (%)	1.28 ± 0.67	0.24 ± 0.41	1.30	-0.06 to 2.14	95.80	-6.59 to 100.00	.060
Heart_V15 (%)	0.37 ± 0.22	0.07 ± 0.16	0.33	0.02-0.66	96.67	5.95-100.00	.069
Heart_V25 (%)	0.06 ± 0.07	0.07 ± 0.10 0.00 ± 0.00	0.04	0.00-0.18	100.00	100.00-100.00	.136
110011 = 1 20 (70)	0.00 _ 0.07	0.00	0.0 1	0.00 0.10	100.00	100.00 100.00	.100

Abbreviations: IMPT, intensity-modulated proton therapy; IMRT, intensity-modulated radiation therapy; SD, standard deviation; WBI, whole breast irradiation; RNI, regional nodal irradiation; IMNI, internal mammary nodes irradiation; Dmean, mean dose; Dmax, maximum dose.

P value is from the paired sample tests of dosimetric parameters between the IMPT and IMRT.

using MHD or LV_V5 differs. In left-sided RNI with IMNI, IMPT reduces individual ACE risk, ranging from 0.51% to 0.88% based on LV_V5 (P=.002) and ranging from 0.19% to 2.75% based on MHD (P=.0015). For right-sided patients, LV_V5 reaches zero, whereas using the MHD model, there remains a borderline significant benefit from IMPT in right-sided RNI with and without IMNI (P=.058 and .063, respectively). For example, a right-sided patient (P=.018) with multiple cardiovascular risk factors undergoing RNI without IMN can achieve up to a 1.27% reduction in ACE risk with IMPT (Table S3).

Cardiovascular risk factors significantly influence the benefits of IMPT in reducing ACE risk, and the degree of benefit from IMPT

increases when more cardiovascular risk factors are found in 1 patient. Assuming the patient has cardiovascular risk factors or an ACE risk score of 4, the predicted reduction in ACE risk would significantly increase according to both the Darby et al⁸ model and the van den Bogaard et al³⁸ model (Table S4).

Discussion

Although there is little controversy that IMPT is associated with a significant reduction in heart radiation exposure in patients receiving breast RT using state-of-the-art photon techniques, there is a lack of a

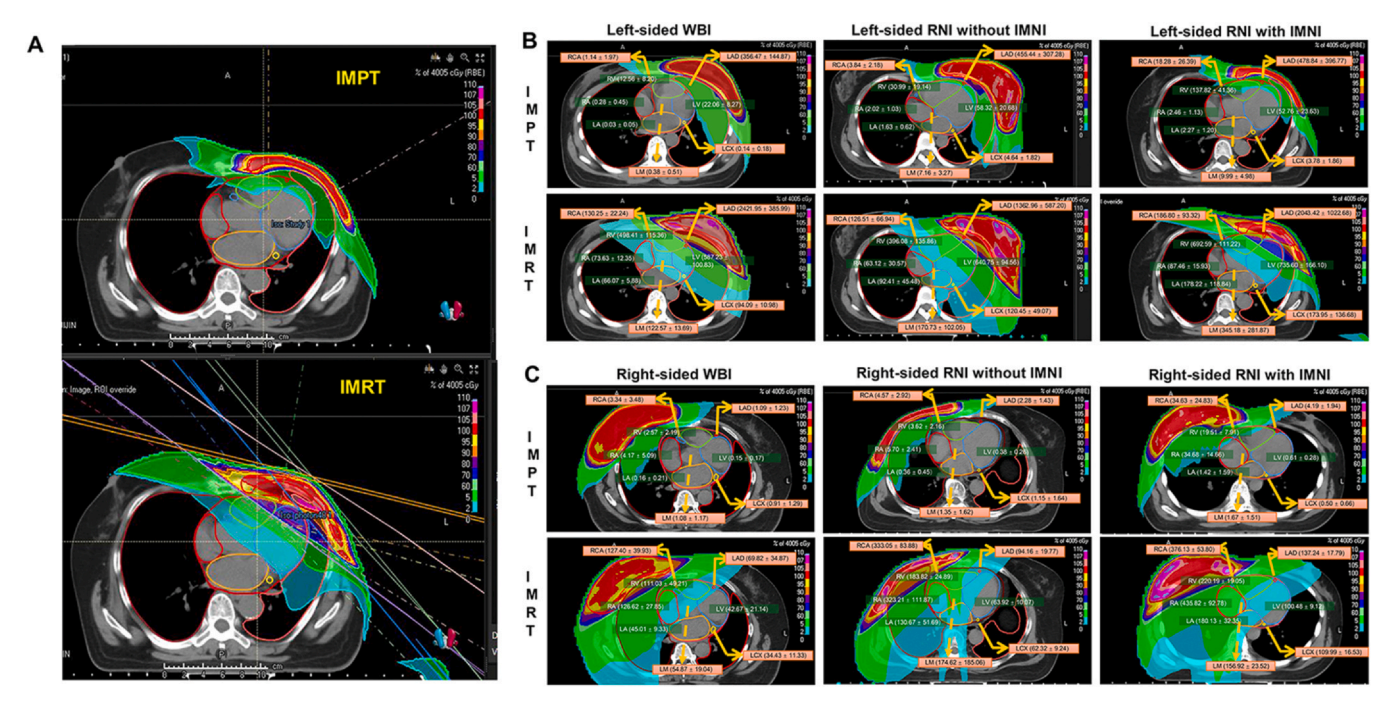


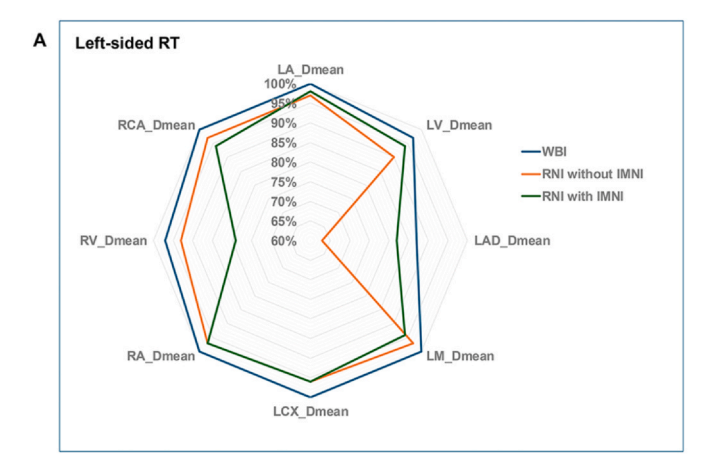
Figure 1. The irradiation field diagrams of IMPT and IMRT (A) and illustration of cardiac substructures delineation, mean dose, and isodose line distribution for IMPT and IMRT in left-sided (B) and right-sided (C) patients. Note: The mean dose to cardiac substructures is measured in cGy(RBE). The left main coronary artery is not present in the displayed CT slice and is indicated as a positional reference. Abbreviations: IMNI, internal mammary node irradiation; IMPT, intensity-modulated proton therapy; IMRT, intensity-modulated radiation therapy; RNI, regional nodal irradiation; and WBI, whole breast irradiation.

panorama view to compare cardiac substructures dose with IMPT and IMRT. To our knowledge, this study is the first to carry on for that particular purpose. In selected patients with high MHD using IMRT, IMPT significantly reduces doses to all cardiac substructures, with variations depending on tumor laterality and target volume. Left-sided patients benefit from a higher absolute dose reduction, while right-sided patients show a greater relative reduction. IMPT reduces dose more significantly in substructures distal to the target volume. Therefore, for left-sided patients, the remaining doses are concentrated in the LAD LV and RV, especially in RNI with IMN. Right-sided patients had only minimal residual dose to the RA, RV, and RCA. NTCP models indicate the significant benefits of IMPT over IMRT in reducing ACE risk, particularly for left-sided patients and those with cardiovascular risk factors.

In our selected patient cohort, MHD was 563.31 ± 65.28 and 424.28 ± 60.05 cGy in left-sided patients with and without IMNI using

IMRT, respectively. With IMPT, the corresponding MHDs were 76.97 \pm 10.62 and 66.31 \pm 25.88 cGy(RBE), respectively, which is consistent with previous research. $^{25,39-43}$ For example, Oonsiri et al 39 reported similar MHD with and without IMNI when using IMPT (110 cGy[RBE] and 120 cGy[RBE], respectively). Given the growing evidence of survival and recurrence control benefits of including IMNI in RNI, 2,3,44,45 our results suggest that IMPT could be a therapeutic strategy worth recommending when IMNI is indicated.

Our study identified significant dose reductions to all cardiac substructures with IMPT compared to IMRT. Mast et al ⁴² found that IMPT significantly reduced the mean dose, V5, and V20 of the LAD compared to tangential IMRT with deep inspiration breath-hold in 20 left-sided WBI patients. Additionally, in 14 left-sided patients undergoing IMNI, IMPT significantly reduced doses to the LV, RV, and LAD compared to volumetric modulated arc therapy (VMAT). ⁴⁶ However, the magnitude of dose reduction across different cardiac substructures differs, as



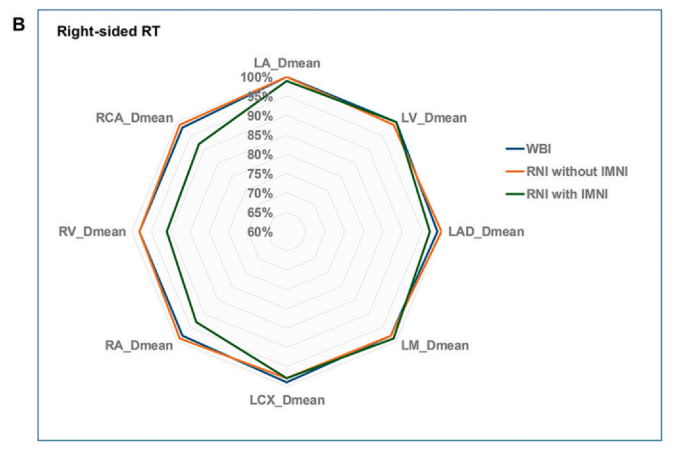


Figure 2. Percentage reduction in mean dose to cardiac substructures with IMPT compared to IMRT in left-sided (A) and right-sided (B) patients. Abbreviations: IMNI, internal mammary node irradiation; LA, left atrium; LAD, left anterior descending coronary artery; LCX, left circumflex coronary artery; LM, left main coronary artery; LV, left ventricle; RA, right atrium; RCA, right coronary artery; RNI, regional nodal irradiation; RV, right ventricle; and WBI, whole breast irradiation.

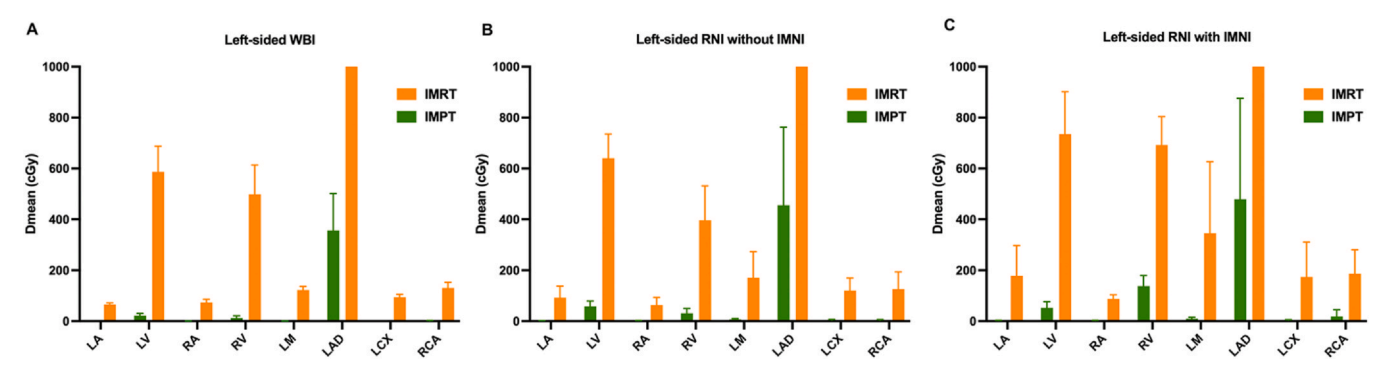


Figure 3. The mean dose to cardiac substructures with the use of IMPT and IMRT in left-sided patients treated with WBI (A), RNI without IMNI (B), and RNI with IMNI (C). Abbreviations: IMNI, internal mammary node irradiation; IMPT, intensity-modulated proton therapy; IMRT, intensity-modulated radiation therapy; LA, left atrium; LAD, left anterior descending coronary artery; LCX, left circumflex coronary artery; LM, left main coronary artery; LV, left ventricle; RA, right atrium; RCA, right coronary artery; RNI, regional nodal irradiation; RV, right ventricle; and WBI, whole breast irradiation.

revealed by our study. The benefits of IMPT are primarily influenced by tumor laterality and target volume. Dose reduction was most pronounced in substructures distal to the target volume, which is also usually at the distal part of the proton beam range, RA, RV, RCA, LM, LCX, and left atrium in left-sided RNI, particularly in those involving IMNI. In right-sided patients without IMNI, most cardiac substructures saw over a 90% reduction in mean doses to 5 cGy(RBE). However, with IMNI, right-sided structures like the RA, RV, and RCA showed smaller reductions, especially in maximum doses. Furthermore, we found no significant correlation in mean and maximum dose reductions across the whole heart and cardiac substructures for both left- and right-sided patients. This can be explained by the difference in beam arrangement with IMPT and IMRT (Figure 1A).

Previous research has primarily concentrated on the LV and LAD due to their proximity to left-sided tangential-based fields.²⁵ However, it is essential to recognize that all cardiac substructures are vulnerable to radiation damage, with different clinical manifestations.^{6,47} In our earlier study on IMRT,²⁹ we found that the LAD, LV, and RV received the highest doses for left-sided patients, while the RA, RCA, and RV were most irradiated for right-sided patients. Similarly, Milo et al²⁶ observed the highest RT doses in the LV and LAD for left-sided RT and the RA and RCA in right-sided RT using photon therapy. In this study, we further observed that

with IMPT, the residual mean dose was concentrated on LV, LAD, and RV for left-sided patients, especially in RNI with IMNI cases. As modern RT techniques reduce overall cardiac risk, previously overshadowed toxicities may show their clinical meaning. Increasing attention is being paid to cardiac conduction system dysfunction. 31,33,48 In our previous analysis of cardiac toxicity in patients treated with a combination of postoperative RT and anti-HER2 therapy, we observed that the rate of conduction system dysfunction (60.3%) was significantly higher than other cardiac events, including left ventricular ejection fraction decline (0.6%), left ventricular diastolic dysfunction (7.5%) and NT-proBNP abnormalities (7.4%).⁴⁹ This dysfunction possibly originates from radiation-induced toxicity affecting the sinus and atrioventricular nodes located in the RA and RV. 50 Although IMPT can decrease cardiac exposure compared to IMRT in general, in addition to focusing on left-sided structures such as the LV and LAD, attention should also be paid to right-sided substructures, including sinus and atrioventricular nodes. The availability of delineation atlases for the cardiac conduction system provides valuable tools for evaluating the impact of radiation on these structures, making dose assessment for the cardiac conduction system more feasible.⁵¹ Studies to evaluate the cardiac protective strategy with proton therapy need to expand their scope for better understanding and mitigating the risks of conduction disorders following thoracic RT.

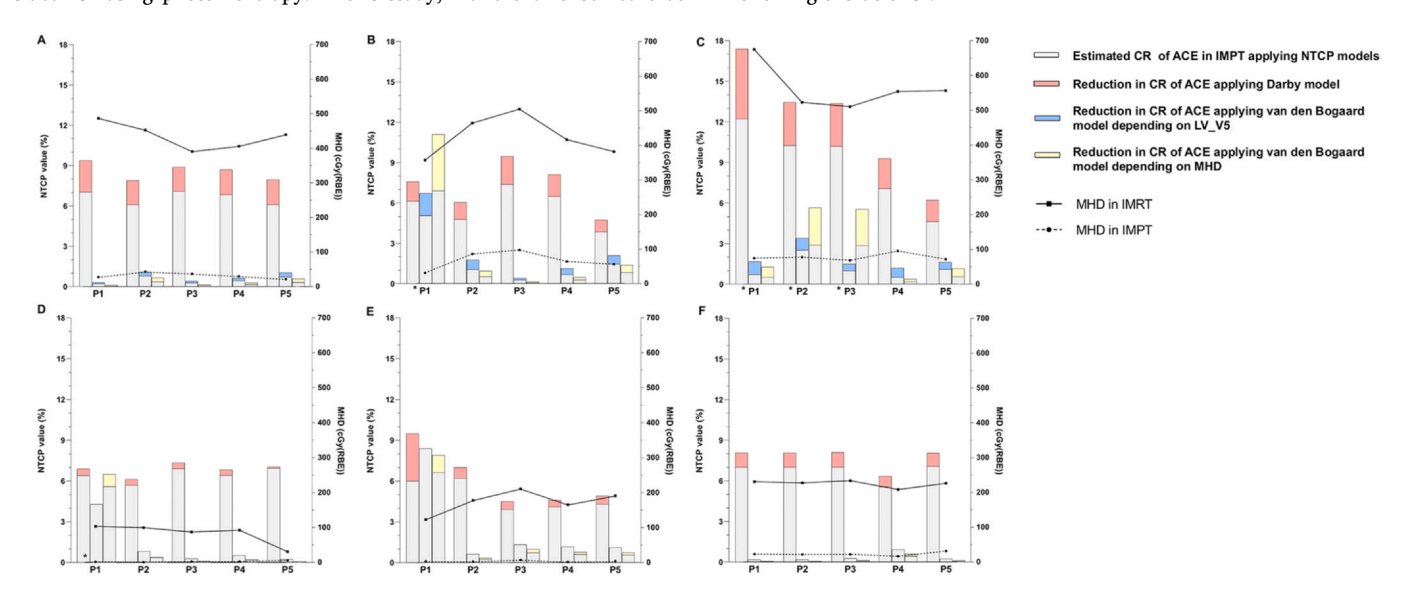


Figure 4. Reduction in estimated cumulative risk of acute coronary event in IMPT applying NTCP models, case by case, in left-sided WBI (A), left-sided RNI without IMNI (B), left-sided RNI with IMNI (C), right-sided WBI (D), right-sided RNI without IMNI (E), and right-sided RNI with IMNI (F). Note: Patients with cardiovascular risk factors were marked by *; The estimated cumulative risk of ACE in IMPT equals the estimated cumulative risk of ACE in IMPT plus the reduction in the estimated cumulative risk of ACE. Abbreviations: CR, cumulative risk; IMPT, intensity-modulated proton therapy; IMRT, intensity-modulated radiation therapy; MHD, mean heart dose; and NTCP, normal tissue complication probability.

Although radiation-induced heart diseases are closely linked to radiation dose, ^{52,53} NTCP models for predicting these risks remain scarce. The proton therapy working group for breast cancer in the Netherlands identified the Darby et al⁸ model as the sole model meeting the national indication protocol for proton therapy criteria for model-based selection of breast cancer patients.²⁴ Using the Darby et al⁸ model, our study found a significant reduction in ACE risk with IMPT, especially in leftsided patients or those with cardiovascular risk factors. Interestingly, IMNI did not significantly alter the estimated risk reduction, likely due to the minimal difference in MHD between patients with and without IMNI with IMRT in our cohort. Building on the Darby et al⁸ model, van den Bogaard et al³⁸ developed a modified NTCP model to predict the cumulative ACE risk within 9 years, based on MHD or LV_V5. Their findings indicate that the ACE risk predictions using MHD are consistent with existing literature, while LV V5 serves as a better predictor.³⁸ Using the van den Bogaard et al³⁸ model, our cohort observed a significant difference in estimated ACE risk based on MHD and LV V5. For left-sided patients without cardiovascular risk factors, ACE risk reduction with IMPT based on LV V5 was generally greater than that based on MHD. However, for patients with risk factors, MHD-based risk reduction was more pronounced. Assuming all patients have risk factors, IMPT offers substantial ACE risk reduction benefits, whether using the Darby model or the van den Bogaard et al³⁸ model. For right-sided patients, only the MHD-based model showed the ACE risk reduction benefit of IMPT. These findings suggest that IMPT can mitigate ACE risk by reducing heart irradiation doses, with the most significant benefits observed in left-sided patients and those with cardiovascular risk factors. However, existing NTCP models primarily focus on LAD events. There is also a lack of NTCP models based on dose metrics for other substructures. A comprehensive NTCP model for integrating cardiac substructure dose, patient-specific characteristics, and treatment-related factors will be ideal for decision-making regarding proton therapy. The introduction of artificial intelligence will give the possibility to integrate vast data sets and, therefore, make the model possible. Nevertheless, the estimated cardiac toxicity reduction with IMPT calculated using NTCP models requires validation through long-term clinical follow-up data.

In our study, robustness optimization is implemented to address setup and range uncertainties. However, respiratory motion introduces additional complexities in proton therapy due to density variations during the breathing cycle. Although 4D CT imaging helps to manage motion-related uncertainties, the interplay between respiratory dynamics and robustness optimization requires further investigation. Additionally, daily setup variations and anatomical changes can impact dose accuracy to different degrees. Image-guided radiation therapy or surface-guided radiation therapy may improve setup reproducibility and robustness, warranting further exploration to optimize dose delivery under motion-related uncertainties. Moreover, LET-based optimization was not utilized in the IMPT optimization in this study. With en-face proton beams, range uncertainties and elevated LET near the end of the range could potentially increase the biological dose to critical substructures such as the LAD in left-sided cases. Future studies are needed to explore LET-based optimization strategies to enhance the safety and effectiveness of IMPT.

Limitations

Despite the data being based on a prospective clinical trial, the small sample size may introduce bias. The variability in cardiac toxicity risk reduction among different target volumes suggests the limitation of the available NTCP models, which currently focus on MHD or LV and use ACE risk as the only endpoint. This may overlook individual cardiac toxicity risks, especially for right-sided patients, such as cardiac conduction system dysfunctions. Finally, our assessment of the cardiac toxicity benefits of IMPT relies on NTCP models rather than long-term follow-up data, emphasizing the need for future studies to validate these findings with empirical evidence.

Conclusions

In conclusion, our study demonstrates that IMPT significantly reduces the dose to all cardiac substructures compared to IMRT, irrespective of tumor laterality and target volume. The reduction in cardiac toxicity risk associated with IMPT is most notable among left-sided patients with RNI and those with cardiac risk factors. There is a need for long-term clinical follow-up data to establish a comprehensive cardiac toxicity profile corresponding to different substructure doses to optimize the current NTCP model based solely on ACE as the endpoint.

Ethics

This study was approved by the local ethics committees of the participating institutions, and informed consent was obtained from all patients.

Funding

This study was supported in part by the National Natural Science Foundation of China (grant numbers 82373202 and 82373514), Noncommunicable Chronic Diseases-National Science and Technology Major Project (grant numbers 2023ZD0502200 and 2023ZD0502206), Shanghai Science and Technology Innovation Action Plan (grant number 23Y41900100), National Key Research and Development Program of China (grant number 2022YFC2404602), Clinical Research of Shanghai Municipal Health Commission (grant number 20224Y0025), Shanghai Hospital Development Center Foundation (grant number SHDC12023108), and Shanghai Science and Technology Innovation Action Plan Natural Science Fund Project (grant number 24ZR1446900). The funding sources had no role in the study design, data collection, data analysis, data interpretation, or writing of the report.

Author Contributions

Conception/design: J.C., L.C. Provision of study material or patients: H.Z., S.Z., K.L., J.Y., G.C., H.L., F.X., W.Q. Collection and/or assembly of data: H.Z., M.C., J.Y., D.O., Y.-B.Z. Data analysis and interpretation: L.C., H.Z., S.Z., K.L., X.W. Manuscript writing: J.C., L.C., H.Z., S.Z., K.L., Final approval of manuscript: All authors.

Data availability

Summary data will be made available upon reasonable request by email to the corresponding author.

Declaration of Conflicts of Interest

The authors declare that they have no known competing financial interests or personal relationships that could have appeared to influence the work reported in this paper.

Appendix A. Supplementary material

Supplementary material associated with this article can be found in the online version at doi:10.1016/j.ijpt.2025.100752.

References

- Bray F, Laversanne M, Sung H, et al. Global cancer statistics 2022: GLOBOCAN estimates of incidence and mortality worldwide for 36 cancers in 185 countries. CA: Cancer J Clin. 2024;74:229–263.
- Early Breast Cancer Trialists' Collaborative Group (EBCTCG). Radiotherapy to regional nodes in early breast cancer: an individual patient data meta-analysis of 14 324 women in 16 trials. *Lancet*. 2023;402:1991–2003.
- McGale P, Taylor C, Correa C, et al. Effect of radiotherapy after mastectomy and axillary surgery on 10-year recurrence and 20-year breast cancer mortality: meta-

- analysis of individual patient data for 8135 women in 22 randomised trials. *Lancet.* 2014;383:2127–2135
- Darby S, McGale P, Correa C, et al. Effect of radiotherapy after breast-conserving surgery on 10-year recurrence and 15-year breast cancer death: meta-analysis of individual patient data for 10,801 women in 17 randomised trials. *Lancet*. 2011;378:1707–1716.
- Henson KE, McGale P, Darby SC, et al. Cardiac mortality after radiotherapy, chemotherapy and endocrine therapy for breast cancer: cohort study of 2 million women from 57 cancer registries in 22 countries. *Int J Cancer*. 2020;147:1437–1449.
- Meattini I, Poortmans PM, Aznar MC, et al. Association of breast cancer irradiation with cardiac toxic effects: a narrative review. JAMA Oncol. 2021;7:924–932.
- Bates JE, Chen MH, Constine LS. Radiation-associated coronary disease in young cancer survivors: the beat goes on; we must preserve it. JACC CardioOncol. 2021;3:393–396.
- Darby SC, Ewertz M, McGale P, et al. Risk of ischemic heart disease in women after radiotherapy for breast cancer. N Engl J Med. 2013;368:987–998.
- Preston DL, Shimizu Y, Pierce DA, et al. Studies of mortality of atomic bomb survivors. Report 13: solid cancer and noncancer disease mortality: 1950-1997. Radiat Res. 2003:160:381–407.
- Munshi A, Jain A, Jalali R, Budrukar A. In regards to Carr et al.: coronary artery disease after radiotherapy for peptic ulcer disease (Int J Radiat Oncol Biol Phys 2005;61:842-850). Int J Radiat Oncol Biol Phys. 2006;65:957 author reply 957.
- Carr ZA, Land CE, Kleinerman RA, et al. Coronary heart disease after radiotherapy for peptic ulcer disease. Int J Radiat Oncol Biol Phys. 2005;61:842–850.
- Loap P, Kirov K, Kirova Y. Cardiotoxicity in breast cancer patients treated with radiation therapy: from evidences to controversies. Crit Rev Oncol Hematol. 2020;156:103121.
- Hassan MZO, Awadalla M, Tan TC, et al. Serial measurement of global longitudinal strain among women with breast cancer treated with proton radiation therapy: a prospective trial for 70 patients. Int J Radiat Oncol Biol Phys. 2023;115:398–406.
- Karasawa K, Omatsu T, Murata K, et al. Clinical trials of carbon ion radiotherapy for early-stage breast cancer. Int J Radiat Oncol Biol Phys. 2023;117:e183.
- Yu B, Li K-W, Fan Y, Pei X. Value of carbon-ion radiotherapy for breast cancer. Int J Part Ther. 2024;14:100629.
- Haefner MF, Verma V, Bougatf N, et al. Dosimetric comparison of advanced radiotherapy approaches using photon techniques and particle therapy in the postoperative management of thymoma. Acta Oncol. 2018;57:1713–1720.
- Barcellini A, Rordorf R, Dusi V, et al. Pilot study to assess the early cardiac safety of carbon ion radiotherapy for intra- and para-cardiac tumours. Strahlenther Onkol. 2024;200:1080–1087
- Berlin E, Yegya-Raman N, Hollawell C, et al. Breast reconstruction complications after postmastectomy proton radiation therapy for breast cancer. Adv Radiat Oncol. 2024;9:101385.
- Mutter RW, Giri S, Fruth BF, et al. Conventional versus hypofractionated postmastectomy proton radiotherapy in the USA (MC1631): a randomised phase 2 trial. Lancet Oncol. 2023;24:1083–1093.
- Hartsell WF, Simone CB, 2nd, et al. Temporal evolution and diagnostic diversification of patients receiving proton therapy in the United States: a ten-year trend analysis (2012 to 2021) from the National Association for Proton Therapy. Int J Radiat Oncol Biol Phys. 2024;119:1069–1077.
- Tambas M, van der Laan HP, Steenbakkers Rjhm, et al. Current practice in proton therapy delivery in adult cancer patients across Europe. Radiother Oncol. 2022;167:7–13.
- Stick LB, Lorenzen EL, Yates ES, et al. Selection criteria for early breast cancer patients in the DBCG proton trial the randomised phase III trial strategy. Clin Transl Radiat Oncol. 2021;27:126–131.
- Fuglsang Jensen M, Stick LB, Høyer M, et al. Proton therapy for early breast cancer
 patients in the DBCG proton trial: planning, adaptation, and clinical experience from
 the first 43 patients. *Acta Oncol.* 2022;61:223–230.
- Boersma LJ, Sattler MGA, Maduro JH, et al. Model-based selection for proton therapy in breast cancer: development of the national indication protocol for proton therapy and first clinical experiences. Clin Oncol. 2022;34:247–257.
- Costin IC, Cinezan C, Marcu LG. Cardio-oncology concerns in radiotherapy: heart and cardiac substructure toxicities from modern delivery techniques. Crit Rev Oncol Hematol. 2024;204:104538.
- Holm Milo ML, Slot Møller D, Bisballe Nyeng T, et al. Radiation dose to heart and cardiac substructures and risk of coronary artery disease in early breast cancer patients: a DBCG study based on modern radiation therapy techniques. *Radiother Oncol.* 2023;180:109453.
- Eber J, Schmitt M, Dehaynin N, et al. Evaluation of cardiac substructures exposure of DIBH-3DCRT, FB-HT, and FB-3DCRT in hypofractionated radiotherapy for left-sided breast cancer after breast-conserving surgery: an in silico planning study. Cancers. 2023;15(13):3406.

- 28. Wolf J, Stoller S, Lübke J, et al. Deep inspiration breath-hold radiation therapy in left-sided breast cancer patients: a single-institution retrospective dosimetric analysis of organs at risk doses. Strahlenther Onkol. 2023;199:379–388.
- Cao L, Ou D, Qi WX, et al. A randomized trial of early cardiotoxicity in breast cancer
 patients receiving postoperative IMRT with or without serial cardiac dose constraints. Int J Cancer. 2025;156(6):1213–1224.
- Niska JR, Thorpe CS, Allen SM, et al. Radiation and the heart: systematic review of dosimetry and cardiac endpoints. Expert Rev Cardiovasc Ther. 2018;16:931–950.
- Tadic M, Kersten J, Buckert D, et al. Right ventricle and radiotherapy: more questions than answers. *Diagnostics*. 2023;13(1):164.
- Pedersen LN, Schiffer W, Mitchell JD, Bergom C. Radiation-induced cardiac dysfunction: practical implications. Kardiol Pol. 2022;80:256–265.
- Errahmani MY, Locquet M, Spoor D, et al. Association between cardiac radiation exposure and the risk of arrhythmia in breast cancer patients treated with radiotherapy: a case-control study. Front Oncol. 2022;12:892882.
- 34. Feng Mary, Moran Jean M, Koelling Todd, et al. Development and validation of a heart atlas to study cardiac exposure to radiation following treatment for breast cancer. Int J Radiat Oncol Biol Phys. 2011;79:10–18.
- Radiation Therapy Oncology Group. Breast cancer contouring atlas. Available from: (http://www.rtog.org/Corel.ab/ContouringAtlases/BreastCancerAtlas.aspx).
- Zhang M, Cao L, Chen J, et al. Mapping of PET/CT-based regional nodes distribution
 of recurrent/advanced breast cancer and comparison with current delineation atlas.

 Br J Radiol. 2022;95:20220382.
- Ma J, Li J, Xie J, et al. Post mastectomy linac IMRT irradiation of chest wall and regional nodes: dosimetry data and acute toxicities. Radiat Oncol. 2013;8:81.
- **38.** van den Bogaard VA, Ta BD, van der Schaaf A, et al. Validation and modification of a prediction model for acute cardiac events in patients with breast cancer treated with radiotherapy based on three-dimensional dose distributions to cardiac substructures. *J Clin Oncol.* 2017;35:1171–1178.
- Oonsiri P, Nantavithya C, Lertbutsayanukul C, et al. Dosimetric evaluation of photons versus protons in postmastectomy planning for ultrahypofractionated breast radiotherapy. *Radiat Oncol.* 2022;17:20.
- Ko H, Chang JS, Moon JY, et al. Dosimetric comparison of radiation techniques for comprehensive regional nodal radiation therapy for left-sided breast cancer: a treatment planning study. Front Oncol. 2021;11:645328.
- Hernandez M, Zhang R, Sanders M, Newhauser W. A treatment planning comparison of volumetric modulated arc therapy and proton therapy for a sample of breast cancer patients treated with post-mastectomy radiotherapy. *J Proton Ther*. 2015;1(1):119.
- Mast ME, Vredeveld EJ, Credoe HM, et al. Whole breast proton irradiation for maximal reduction of heart dose in breast cancer patients. *Breast Cancer Res Treat*. 2014;148:33–39.
- MacDonald SM, Jimenez R, Paetzold P, et al. Proton radiotherapy for chest wall and regional lymphatic radiation; dose comparisons and treatment delivery. Radiat Oncol. 2013;8:71
- 44. Thorsen LBJ, Overgaard J, Matthiessen LW, et al. Internal mammary node irradiation in patients with node-positive early breast cancer: fifteen-year results from the Danish Breast Cancer Group Internal Mammary Node Study. J Clin Oncol. 2022;40:4198–4206.
- Recht A. Internal mammary node irradiation debate: case closed? Not yet, and maybe never. J Clin Oncol. 2024;42:1871–1874.
- 46. Loap P, Tkatchenko N, Goudjil F, et al. Cardiac substructure exposure in breast radiotherapy: a comparison between intensity modulated proton therapy and volumetric modulated arc therapy. Acta Oncol. 2021;60:1038–1044.
- Bergom C, Bradley JA, Ng ÅK, et al. Past, present, and future of radiation-induced cardiotoxicity: refinements in targeting, surveillance, and risk stratification. *JACC CardioOncol.* 2021;3:343–359.
- Domanský M, Kubeš J. Cardiac conduction system as a new organ at risk in radiotherapy. Klin Onkol. 2024;38:10–19.
- 49. Yang J, Zhou MY, Yu B, et al. A multicenter retrospective study of early cardiac toxicity in operable breast cancer patients receiving concurrent dual or mono anti-HER2 therapy with postoperative radiation therapy. *Breast*. 2025;79:103879.
- Loap P, Goudjil F, Servois V, et al. Radiation exposure of cardiac conduction nodes during breast proton therapy. Int J Part Ther. 2023;10:59–64.
- Loap P, Servois V, Dhonneur G, et al. A radiation therapy contouring atlas for cardiac conduction node delineation. Pract Radiat Oncol. 2021;11:e434–e437.
- Lai TY, Hu YW, Wang TH, et al. Association of radiation dose to cardiac substructures with major ischaemic events following breast cancer radiotherapy. Eur Heart J. 2023;44:4796–4807.
- Aznar M, Nohria A. Reducing radiation to the heart in breast cancer: is that all that matters? Eur Heart J. 2023;44:4807–4809.